



## Seminar Paper

Weiqi Yin (tcj327)

# **Which Volatility Model Captures the Observed Implied Volatility Smile under the 2008 and 2020 Global Market Crash?**

-The Case of S&P 500 Index Option

Course: 2020 Spring Financial Theory and Models

Teacher: Frank Hansen

ETCS Points:7.5

Submitted on: June 2,2020

Standard Page: 13 Pages

# Contents

<b>1</b>	<b>Introduction</b>	<b>1</b>
<b>2</b>	<b>Black-Scholes-Merton (BSM) Model and its Discontents</b>	<b>2</b>
2.1	Black-Scholes-Merton (BSM) Model . . . . .	2
2.2	Implied Volatility Smile . . . . .	3
<b>3</b>	<b>SABR model and Merton jump-diffusion model</b>	<b>4</b>
3.1	SABR model . . . . .	5
3.2	Jump-Diffusion Models . . . . .	6
<b>4</b>	<b>Empirical Analysis</b>	<b>7</b>
4.1	Calibration . . . . .	7
4.2	Empirical Result . . . . .	8
4.2.1	2008 Market Crash . . . . .	9
4.2.2	2020 Market Crash . . . . .	11
<b>5</b>	<b>Discussion</b>	<b>12</b>
<b>6</b>	<b>Conclusion</b>	<b>13</b>
<b>A</b>	<b>Appendix</b>	<b>15</b>
A.1	Proof of Implied volatility under ATM option in SABR model . . . . .	15
A.2	Proof of PIDE in Merton Jump-diffusion model . . . . .	15
A.3	Proof of Characteristic Function for Merton Jump-diffusion Model . . . . .	16
A.4	Proof of Pricing Formula for Merton Jump-diffusion Model . . . . .	17
A.5	2008 Market Crash Original Data . . . . .	20
A.5.1	Calibrated SABR Data . . . . .	20
A.5.2	Calibrated Merton Jump-diffusion Data . . . . .	20
A.6	2020 Market Crash Original Data . . . . .	21
A.6.1	Calibrated SABR Data . . . . .	21
A.6.2	Calibrated Merton Jump-diffusion Data . . . . .	21

# Which Volatility Model Captures the Observed Implied Volatility Smile under the 2008 and 2020 Global Market Crash?

## -The Case of S&P 500 Index Option

Weiqi Yin

June 2, 2020

### Abstract

In this seminar paper, we examine SABR model and Merton jump-diffusion model's calibrated effectiveness on capturing the S&P 500 index option's volatility smile and skew under the 2008 and 2020 market crash. Our empirical result shows that SABR model overall calibrates the volatility smile and skew better than Merton jump-diffusion model. However, the unrealistic calibrated parameter values in SABR model challenges its calibrated effectiveness.

## 1 Introduction

In the option pricing, Black and Scholes (1973) apply the partial differential equation to describe the evolution of a derivative's price over time, which is known as the Black-Scholes formula. Black-Scholes formula offers a theoretical European-style option price. The success of the Black-Scholes formula booms the option trading market. In the Black-Scholes-Merton (BSM) model framework, the volatility is assumed to be constant over time. Prior to the 1987 market crash, BSM model describes the option market fairly well. A plot of the volatility with the same time-to-expiration but with different strike prices displays a flat line. This is consistent with the BSM model assumption. However, after the crash, the equity index option displays a volatility smile or skew, which means the volatility is not constant over time. Such inconsistency also happens in the non-market crash period. The presence of volatility smiles and skews challenges the BSM model's validity.

After that people propose more promising models to account for the volatility smile and skew. In this seminar paper, we introduce the SABR model and the Merton jump-diffusion model to capture the volatility smile. SABR model is a model in which volatility is driven by another stochastic process and the volatility stochastic process accounts for the volatility smile and skew. Merton jump-diffusion model allows the underlying asset price to make arbitrary jumps. Arbitrary jumps on underlying asset generate the volatility smile and skew. We employ those two models to see their effectiveness during the 2008 and 2020 market crash. We take S&P 500 index option as an example.

This paper is organized as follows. Section 2 describes Black-Scholes-Merton (BSM) model and its discontents. SABR model and Merton jump-diffusion model are presented in section 3. We analyze and compare those two models in section 4. Section 5 is the discussion part and section 6 concludes the paper.

## 2 Black-Scholes-Merton (BSM) Model and its Discontents

Black-Scholes-Merton (BSM) model is an option pricing model introduced by Black and Scholes (1973) and Merton (1973). It is one of the widely used option pricing models around the world. In this section, we derivate the BSM model based on (Hull (2013), p309) work and discuss one of the problems that the BSM model cannot cope with which is the volatility smile.

### 2.1 Black-Scholes-Merton (BSM) Model

A Call option is a financial contract that gives a holder a right, but not an obligation to buy an underlying asset at an appointed price prior to or on a specific date. A European option is a not path-dependent option which gives a holder a right to exercise an option at a specified date. Pricing a European call option is a problem about solving the differential equation. Black and Scholes (1973) and Merton (1973) apply the partial differential equation (PDE), a differential equation that involves multivariable functions and their partial derivatives to describe the evolution of an option price over time. Denote underlying non-dividend asset price at time  $t$  is  $S_t$  and  $K$  is the strike price.  $T$  is the expire time, then the time to maturity  $\tau$  is equal to  $T - t$ .

In the BSM model, we assume the underlying asset price  $S_t$  follows a geometric Brownian motion:

$$\frac{dS_t}{S_t} = \mu dt + \sigma dW_t \quad (2.1)$$

where  $\mu$  is constant drift and  $\sigma$  is constant volatility.  $W_t$  is a Brownian motion. Denote the  $C$  is a European call option price. From the Ito's lemma, the dynamics of  $C$  is given as:<sup>1</sup>

$$dC = \left( \frac{\partial C}{\partial t} + \frac{\partial C}{\partial S} \mu S + \frac{1}{2} \frac{\partial^2 C}{\partial S^2} \sigma^2 S^2 \right) dt + \frac{\partial C}{\partial S} \sigma S dW \quad (2.2)$$

In equation 2.1 and 2.2, the risk of  $dC$  and  $dS$  is the stochastic term  $dW$ . In order to hedge  $dW$  so that construct portfolio  $\Pi$ , we need to long  $C$  and short  $\frac{\partial C}{\partial S}$  shares of  $S$ . The portfolio  $\Pi$  is given as

$$\Pi = C - \frac{\partial C}{\partial S} S \quad (2.3)$$

Hence, the dynamics of  $\Pi$  is given as

$$d\Pi = dC - \frac{\partial C}{\partial S} dS \quad (2.4)$$

put equation 2.1 and equation 2.2 into equation 2.4 yields.

$$d\Pi = \left( \frac{\partial C}{\partial t} + \frac{1}{2} \frac{\partial^2 C}{\partial S^2} \sigma^2 S^2 \right) dt \quad (2.5)$$

Again,  $d\Pi$  is an instantaneously portfolio and it should earn the risk-free rate  $r$  which means

<sup>1</sup>We will ignore the subscript during the derivation out of simplification.

$$d\Pi = r\Pi dt \quad (2.6)$$

substituting equation 2.3 and equation 2.5 into equation 2.6, we finally have Black-Scholes-Merton PDE:

$$\frac{\partial C}{\partial t} + \frac{\partial C}{\partial S} rS + \frac{1}{2} \frac{\partial^2 C}{\partial S^2} \sigma^2 S^2 = rC \quad (2.7)$$

According to Black and Scholes (1973) and Merton (1973), the solution to the equation 2.7 is :

$$C = S_t \Phi(d_1) - K e^{-rT} \Phi(d_2) \quad (2.8)$$

where

$$d_1 = \frac{\ln(S_t/K) + (r + \frac{\sigma^2}{2})\tau}{\sigma\sqrt{\tau}}$$

$$d_2 = \frac{\ln(S_0/K) + (r - \frac{\sigma^2}{2})\tau}{\sigma\sqrt{\tau}} = d_1 - \sigma\sqrt{\tau}$$

where  $\Phi(\cdot)$  is a cumulative standard normal distribution. Once we obtain all the parameters then we can get a European call option price. Furthermore, the option price is increasing with increasing volatility. This is because the cost of an option holder is fixed. Higher volatility indicates the underlying asset has a high probability of ending up in deep out-of-the-money ( $S_T < K$ ) or deep in-the-money ( $S_T > K$ ). For the call option holder, he can benefit from the extreme price upward movement but experience fixed cost when the price takes the downward movement. Hence, the value of option is an increasing function of volatility.

## 2.2 Implied Volatility Smile

BSM model provides the closed-form solution to price a European call option. However, how to measure the BSM model accuracy. That is how implied volatility comes. According to (Derman and Miller (2016),p131) and Weiqi (2020), implied volatility  $\Sigma(S, K, \tau)$  is the volatility that makes the BSM option price equals to the market price. We can express implied volatility  $\Sigma(S, K, \tau)$  by using the following expression.

$$C^{Market}(S, K, \tau) = C^{BSM}(S, K, T, \Sigma(S, K, \tau)) \quad (2.9)$$

where  $C^{Market}(S, K, \tau)$  is the market option price and  $C^{BSM}(S, K, T, \Sigma(S, K, \tau))$  is the BSM model price. Implied volatility describes the closeness between the BSM model price and the market price. In BSM model, we assume all the call options under the same  $S$  with the same  $\tau$  but with different  $K$  should have the same implied volatility. If BSM model perfectly describes the option market, we should expect that implied volatility with the same  $\tau$  should be constant with different  $K$ .

Prior to the 1987 market crash, A plot of the implied volatility with the same time-to-expiration but with different strike prices display a flat line. This is consistent with BSM model assumption. However, after

the crash, the equity index option displays an implied volatility smile or skew, which means the volatility is not constant. For the implied volatility smile, the volatility in deep-in-the-money option ( $S_T > K$ ) and deep-out-of-the-money option ( $S_T < K$ ) is higher than the at-the-money option ( $S_T = K$ ). In the following section, we define in-the-money, out-of-the-money, and at-the-money as ITM, OTM, and ATM respectively. For the implied volatility skew, a negative implied volatility skew means the implied volatility is decreasing with decreasing strike price  $K$ . Positive volatility skew indicates the implied volatility is increasing with increasing strike price  $K$ . There is no difference for us to describe the implied volatility smile and skew as volatility smile and skew. In the following section, we don't distinguish those terms. After the 1987 market crash, the implied volatility displays a smile or skew even not in the market crash. The presence of the volatility smile and skew challenges the BSM model. To get a better understanding of volatility smile and skew, we employ the implied volatility surface, a three-dimensional graph that describes the implied volatility with different strike prices and time to expiration under the 2008 and 2020 market crash.

2008 market crash is largely attributed to the subprime crisis, S&P 500 index fell by 7.60 % on 15 October 2008, one of the top twenty daily percentage losses in the history. On 9 March 2020, coronavirus pandemic and Russia–Saudi Arabia oil price war made S&P 500 fell by 7.60 %, another top twenty daily percentage losses. Figure 2.1 shows the implied volatility surface on S&P 500 during those two market crash respectively<sup>2</sup>.

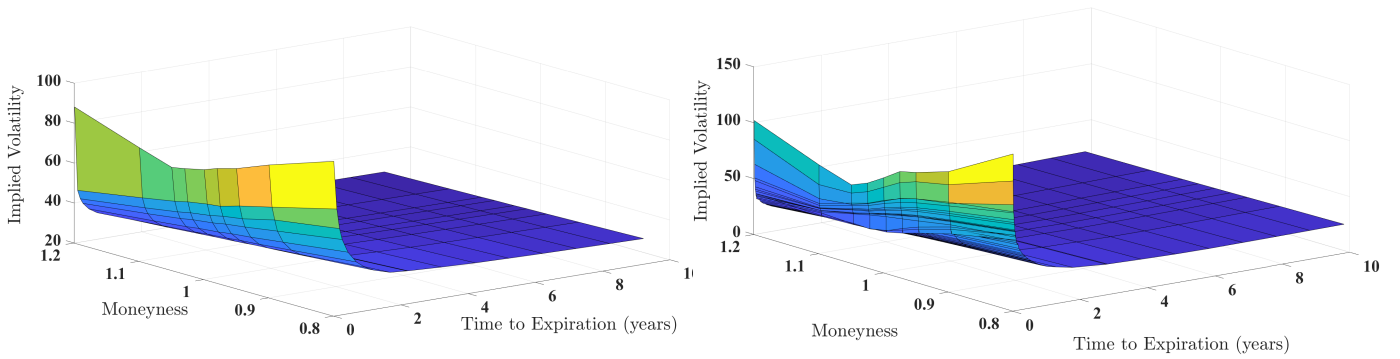


Figure 2.1: S&P 500 Index Option Implied Volatility (in %) under 2008 (Left) and 2020 (Right) Market Crash

From the figure 2.1 we know that the implied volatility exhibits smile and skew with decreasing time to expiration. The implied volatility curve tends to flat in the long expiration. The implied volatility smile and skew in the short expiration challenges the BSM model.

In order to tackle the volatility smile and skew, people try to propose other option pricing models. In our seminar paper, we focus on the stochastic volatility model-SABR model and the jump-diffusion model-Merton model. Those two models relax the BSM model assumption and provide an appealing explanation on volatility smile and skew. In stochastic volatility models, not only the underlying asset follows the stochastic process, but also the volatility. Volatility randomness accounts for the volatility smile. For the jump-diffusion models, the underlying asset can take arbitrary jumps to capture the market crash. The arbitrary jumps in the underlying asset contribute to the volatility smile. We will illustrate it in the following section.

### 3 SABR model and Merton jump-diffusion model

In this section, we introduce SABR model and Merton jump-diffusion model to see how the models generate the implied volatility smile and skew.

<sup>2</sup>We take moneyiness  $\frac{K}{S}$  as x-axis when drawing volatility surface. Taking moneyiness as x-axis allows us to compare the implied volatility under different strike prices with the same time to expiration.

### 3.1 SABR model

In section 2.2, we have shown the volatility is not constant over time. In the stochastic volatility model, the underlying asset volatility  $\sigma$  is driven by another stochastic process. In other words, there are two random processes in the stochastic volatility model, one is the underlying asset and another one is the underlying asset volatility. Those two random processes may correlate with each other because of the leverage effect. In Christie (1982) definition, leverage effect means the underlying asset's volatility is negatively correlated with its price. To illustrate it, we consider one of the stochastic volatility models-SABR model (**S**tochastic **A**lpha, **B**eta, **R**ho model) in Hagan et al. (2002) paper. SABR model is not a model to price an option, but a model to calculate the implied volatility. In SABR model, the underlying asset price  $S_t$  evolves according to

$$\begin{aligned}\frac{dS_t}{S_t} &= \sigma S_t^{\beta-1} W_t^1 \\ d\sigma_t &= \xi \sigma_t dW_t^2 \\ dW_t^1 dW_t^2 &= \rho dt\end{aligned}\tag{3.1}$$

where  $\xi$  represents the volatility of volatility  $\sigma$ .  $\xi$  measures how much smile that the implied volatility displays. Higher  $\xi$  leads the volatility smile more salient and volatile. This implies that the underlying asset price has a greater tendency to take an extreme move, leading to a high option price. Furthermore, (Derman and Miller (2016),p323) argue that the stochastic volatility increases the low- and high-strike options values relative to ATM options, resulting in a volatility smile. How much value is added depending on the parameters value  $\xi$ .

$\beta$  is the power parameter and it is taken  $0 \leq \beta \leq 1$ . The correlation coefficient between the underlying asset price and its corresponding volatility is  $\rho$ , which reflects the leverage effect.  $\rho$  and  $\beta$  control the curve's skew. SABR model can transfer into different patterns with the parameters change. If  $\xi = 0$  and  $\beta = 1$ , the model reduces to the geometric Brownian motion with no smile. If  $\xi = 0$  and  $0 \leq \beta < 1$ , the model reduces to the local volatility model with a skew. In the local volatility case, the volatility is a deterministic function of underlying asset price  $S_t$  and of time  $t$  instead of assuming the constant volatility. When  $\xi \neq 0$  as well as  $0 \leq \beta < 1$ , the model has stochastic volatility and skew.

One of the salient features in SABR model is that it offers a closed-form approximation for the implied volatility. According to Hagan et al. (2002), closed-form approximation for the implied volatility is carried out by applying singular perturbation techniques to price European options, and from these, the implied volatility is then inferred. For the given optimal parameters, the implied volatility  $\sigma^{iv}(S, K)$  is given by<sup>3</sup>:

$$\begin{aligned}\sigma^{iv}(S, K) &= \frac{\sigma_0 \left( 1 + \left( \frac{(1-\beta)^2 \sigma^2}{24(SK)^{1-\beta}} + \frac{\rho \beta \xi \sigma}{4(SK)^{\frac{(1-\beta)}{2}}} + \frac{2-3\rho^2}{24} \xi^2 \right) \tau \right) z}{(SK)^{\frac{(1-\beta)}{2}} \left[ 1 + \frac{(1-\beta)^2}{24} \log^2 \frac{S}{K} + \frac{(1-\beta)^4}{1920} \log^4 \frac{S}{K} + \dots \right] \chi(z)} + \dots \\ z &= \frac{\xi}{\sigma_0} (SK)^{\frac{(1-\beta)}{2}} \log \frac{S}{K} \\ \chi(z) &= \log \left( \frac{\sqrt{1-2\rho z + z^2} + z - \rho}{1 - \rho} \right)\end{aligned}\tag{3.2}$$

where  $\sigma_0$  is the initial volatility. The omitted terms “ $+\dots$ ” are so small that not implement the higher orders does not have a huge impact on the results. In the following, we omit the “ $+\dots$ ” terms since the

<sup>3</sup>Perturbation techniques are well beyond the scope of this seminar paper. In this paper, we mainly focus on the calibrated effectiveness on the SABR model. For that interested, see the derivate details in (Hagan et al. (2002), Appendix B).

increased precision of the higher order results are unnecessary. When the call option is ATM ( $S = K$ ),  $z$  and  $\chi(z)$  are removed from the equation 3.2, then  $\frac{z}{\chi(z)} = 1$  as Hagan et al. (2002) suggest. The equation 3.2 now becomes:

$$\sigma_{ATM}^{iv}(S, S) = \frac{\sigma_0 \left( 1 + \left( \frac{(1-\beta)^2 \sigma^2}{24 S^{2-2\beta}} + \frac{\rho \beta \xi \sigma}{4 S^{1-\beta}} + \frac{2-3\rho^2}{24} \xi^2 \right) \tau \right)}{S^{1-\beta}} \quad (3.3)$$

For the derivation of equation 3.3, we refer to A.1.

### 3.2 Jump-Diffusion Models

One of the assumptions in BSM model is that the underlying asset price moves as geometric Brownian motion. In geometric Brownian motion, underlying asset prices should diffuse smoothly as time passes. However, the underlying asset prices can take the arbitrary number of jumps instead of undergoing the diffusion in geometric Brownian motion. For example, if the S&P 500 index follows the geometric Brownian motion, then the S&P 500 index was not possible to drop 20.47% in a day in the 1987 market crash. The 1987 market crash challenges the geometric Brownian motion and innovates Merton (1976) adds jump into the underlying asset's stochastic process. That is how the Merton jump-diffusion model comes. The jumps account for the observed volatility smile and skew. Unlike the SABR model, jump-diffusion models may explain the extreme steep short-term volatility skew. In Merton jump-diffusion model, the sudden asset price movements are modeled by adding the jump-diffusion parameters with the Poisson process. The dynamics of underlying asset price  $S_t$  is

$$\frac{dS_t}{S_t} = \mu dt + \sigma dW_t + J dq_t \quad (3.4)$$

where  $J$  is the random percentage jump size conditional on the jump occurring and  $q_t$  is a Poisson process. The logarithm of  $J$  also follows a Gaussian distribution

$$\log(1 + J) \sim N \left( \log(1 + \mu_J) - \frac{\sigma_J^2}{2}, \sigma_J^2 \right) \quad (3.5)$$

$\mu_J$  is the mean of the random percentage  $J$  and  $\sigma_J$  is the standard deviation of  $\log(1 + J)$ . In Kovachev (2014) comment,  $\mu_J$  affects the skewness of the underlying asset distribution. Positive  $\mu_J$  generates positive skewness and vice versa.  $\sigma_J$  and  $\lambda$  influences the kurtosis of the underlying asset distribution. Higher  $\sigma_J$  leads to a higher variance in the underlying asset. Higher  $\lambda$  indicates the higher numbers of the jump and leads to higher volatility.

Similar to derivate the PDE in the BSM model, we can also construct the risk-less portfolio, and then through delta-hedging to obtain the partial integro-differential equation (PIDE) in Merton jump-diffusion model if the jump is diversifiable. PIDE is an equation that contains both integrals and function's derivatives. After derivation, the European option price  $C$  in Merton jump-diffusion model satisfies the following partial integro-differential equation.

$$\frac{\partial C}{\partial t} + \frac{1}{2} \frac{\partial^2 C}{\partial S^2} \sigma^2 S^2 + \frac{\partial C}{\partial S} r S - r C + \lambda E \left[ C(S + JS, T) - C(S, t) - \frac{\partial C}{\partial S} JS \right] = 0 \quad (3.6)$$



For the derivation of equation 3.6, we refer to A.2. For  $\lambda = 0$ , there is no jump in the model so that equation reduces to the BSM equation. Unlike the Merton (1976) arguments that the jump-diffusion option price  $C_{JD}$  is a weighted average of BSM option prices. In this seminar paper, we try to solve equation 3.6 by using Fourier transform (characteristic function) methods based on (Gatheral (2011),p56) works. According to (Gatheral (2011),p56), characteristic function  $f^{Merton}(\phi)$  given as:

$$f^{Merton}(\phi) = \exp \left\{ i\phi w\tau - \frac{1}{2}\phi^2\sigma^2\tau + \lambda\tau \left( e^{i\phi \left( \log(1+\mu_J) - \frac{\sigma_J^2}{2} \right) - \frac{\phi^2\sigma_J^2}{2}} - 1 \right) \right\} \quad (3.7)$$

where  $\phi$  is the characteristic function variable and  $i$  is a unit imaginary number which has  $i^2 = -1$ .  $w$  is the drift parameter which has

$$w = -\frac{1}{2}\sigma^2 - \lambda \left( e^{\log(1+\mu_J) + \frac{\sigma_J^2}{2}} - 1 \right) \quad (3.8)$$

For a given characteristic function, European call options can be obtained by using the Fourier transform method as Lewis (2001) suggests

$$C_{JD} = e^{-r\tau} \left\{ S - \sqrt{SK} \frac{1}{\pi} \int_0^\infty \frac{d\chi}{\chi^2 + \frac{1}{4}} \operatorname{Re} \left[ e^{-i\chi k} f^{Merton} \left( \phi = \left( \chi - \frac{i}{2} \right) \right) \right] \right\} \quad (3.9)$$

where  $k = \log \left( \frac{K}{S} \right)$ .  $\chi$  is the characteristic function variable for intergration, where  $\phi = \left( \chi - \frac{i}{2} \right)$ .  $\operatorname{Re}$  is the imaginary function. We can obtain the  $C_{JD}$  by employing numerical integration methods. For the derivation of equation 3.7 and 3.8, we refer to appendix A.3 and the proof of 3.9 is on appendix A.4.

## 4 Empirical Analysis

In this section, we try to compare the calibrated effectiveness between the SABR model and Merton jump-diffusion model in S&P 500 index option during the market crash period. We take the data on October 15, 2008 and March 9, 2020, which are the date within the market crash period. All the data are available on Bloomberg. We provide the data we use in the appendix A.5 and A.6.

### 4.1 Calibration

Before we apply option pricing models into the empirical analysis, we should ensure that the models are feasible. Hence, we need to calibrate the model parameters in order to capture the market data. Assume there are  $N \times M$  European call options exist for a underlying asset, with  $N$  strike price  $K_i, i = 1, 2, \dots, N$  and  $M$  expirations  $T_j, j = 1, 2, \dots, M$ . The goal of calibration is to find the proper parameters that minimize the difference between the model implied volatility  $\sigma^{model}(K_i, T_j)$  and the market implied volatility  $\sigma_i^{Market}(K_i, T_j)$ . We denote  $\Theta$  as the set of parameters we need to calibrate. We need to choose the optimal parameters to minimize the following error function.

$$\min_{\Theta} \sum_{i=1}^N \sum_{j=1}^M [\sigma^{model}(K_i, T_j) - \sigma_i^{Market}(K_i, T_j)]^2 \quad (4.1)$$

Equation 4.1 is applied to calibrate the whole volatility surface. From figure 2.1 we know that the implied volatility displays a smile or a skew in the short expiration and a flat line in the long expiration. The total percentage of flat lines is higher than the skew line in the implied volatility surface. Hence, if we calibrate the whole volatility surface, the calibration process will pay more attention to calibrate the flat lines instead of the skew lines. In other words, it will cause the calibrated ineffectiveness in the skew lines. In order to get the accurate calibrated result, we follow Bogatyreva et al. (2019) and Weiqi (2020) suggestion that calibrating the implied volatility with the different strike prices in the same expiration instead of calibrating the whole volatility surface. The error function now can be written as:

$$\min_{\Theta} \sum_{i=1}^N [\sigma^{model}(K_i) - \sigma^{market}(K_i)]^2 \quad (4.2)$$

Further, calibrating the models involves the multidimensional space. High dimensional space as well as limited data induce inaccurate calibrated results. Therefore, We try to predetermine some parameter values to lower the dimensional space. We take root mean square error (RMSE) as an error measure to measure the model accuracy. RMSE is given as:

$$RMSE = \sqrt{\frac{\sum_{i=1}^N (\sigma_i^{model} - \sigma_i^{market})^2}{N}} \quad (4.3)$$

There are four unknown parameters  $\Theta^{SABR} = \{\sigma_0, \beta, \rho, \xi\}$  in SABR model.  $\{\sigma_0, \beta, \xi\}$  should be nonnegative and  $\rho \in [-1, 1]$ .  $\sigma_0$  determines the overall height of the implied volatility smile and  $\xi$  measures how much smile that the implied volatility displays. Both  $\rho$  and  $\beta$  control the curve's skew. Hence, we need to predetermine the value for one of them. Following Hagan et al. (2002) and West (2005) work, we determine  $\beta$  in advance. Under the specific choice of  $\beta$ , the implied volatility smile that derived from SABR model can match market implied volatility successfully. In Hagan et al. (2002) comment,  $\beta$  cannot be obtained by fitting a implied volatility smile because it will exactly amount to "fitting the noise". We assume  $\beta = 0.5$  since it is fairly reliable and stable in Hagan et al. (2002) work. Even it may unconvincing nowadays, we can also capture the implied volatility by adjusting  $\rho$  because it serves the same role as  $\beta$  does. (Gatheral (2011),p34) suggests  $\sigma_0 = \sigma_{ATM}(\tau)$  where  $\sigma_{ATM}(\tau)$  is the implied volatility of ATM options with expiration  $\tau$ . We follow his setting and make  $\sigma_0 = \sigma_{ATM}(\tau)$ . The unknown parameters in SABR model now become  $\Theta^{SABR} = \{\rho, \xi\}$ .

There are four unknown parameters  $\Theta^{Jump} = \{\sigma_0, \mu_J, \sigma_J, \lambda\}$  in Merton jump-diffusion model.  $\mu_J$  should larger than  $-1$  because it represents the mean of the random percentage  $J$ . The annual jump frequency  $\varpi$  and standard deviation  $\sigma_J$  should be nonnegative. We also set  $\sigma_0 = \sigma_{ATM}(\tau)$  and calibrate three unknown parameters  $\Theta^{Jump} = \{\mu_J, \sigma_J, \lambda\}$  in Merton jump-diffusion model<sup>4</sup>.

To calculate the implied volatility in SABR model, getting the option price under Merton jump-diffusion, and calibrate and parameter values in both models, we use MATLAB to achieve them. In section 4.2, we will discuss both models effectiveness on S&P 500 index options under the market crash.

## 4.2 Empirical Result

Finding the optimal parameters is the process of optimization. In order to find the optimal parameters, we use a nonlinear least-squares method, a method that approximates the model by a linear one and to update

<sup>4</sup>In principle, we should calibrate the same number of parameters in both models for control variate method. However, we try to predetermine the paramter values as much as we can in order to get more accurate result.

the model parameters through continuous iterations. Also, implied volatilities are sensitive to the moneyness  $\frac{K}{S}$  and time to expiration  $\tau$ . In order to make our empirical analysis clearly, we define different moneyness  $\frac{K}{S}$  and  $\tau$  into the following categories based on Weiqi (2020) work:

$$\frac{K}{S} = \begin{cases} \text{Deep out of money (DOTM)} & 0 \leq \frac{K}{S} < 0.95 \\ \text{Out of money (OTM)} & 0.95 \leq \frac{K}{S} \leq 1 \\ \text{At the money (ATM)} & \frac{K}{S} = 1 \\ \text{In the money (ITM)} & 1 < \frac{K}{S} \leq 1.05 \\ \text{Deep in the money (DITM)} & \frac{K}{S} > 1.05 \end{cases} \quad \tau = \begin{cases} \text{Short-term} & 0 \leq \tau < 0.2 \\ \text{Mid-term} & 0.2 < \tau \leq 0.7 \\ \text{Long-term} & \tau > 0.7 \end{cases}$$

In the following analysis, if  $\xi > 1.2$ , we argue that  $\xi$  is unreasonable large or taken extreme value. The underlying reason for us to set this bound is that we have checked previous scholars' work on calibrating the SABR parameter values in S&P 500 index options. The calibrated or initial setting on  $\xi$  is between 0 and 1.2. (Camlibel and Lundgren (2010); Huang (2019))

#### 4.2.1 2008 Market Crash

We calibrate the implied volatility under the 2008 market crash and plot the calibrated result in figure 4.1. The corresponding parameters and  $RMSE$  are shown in table 4.1 and 4.2.

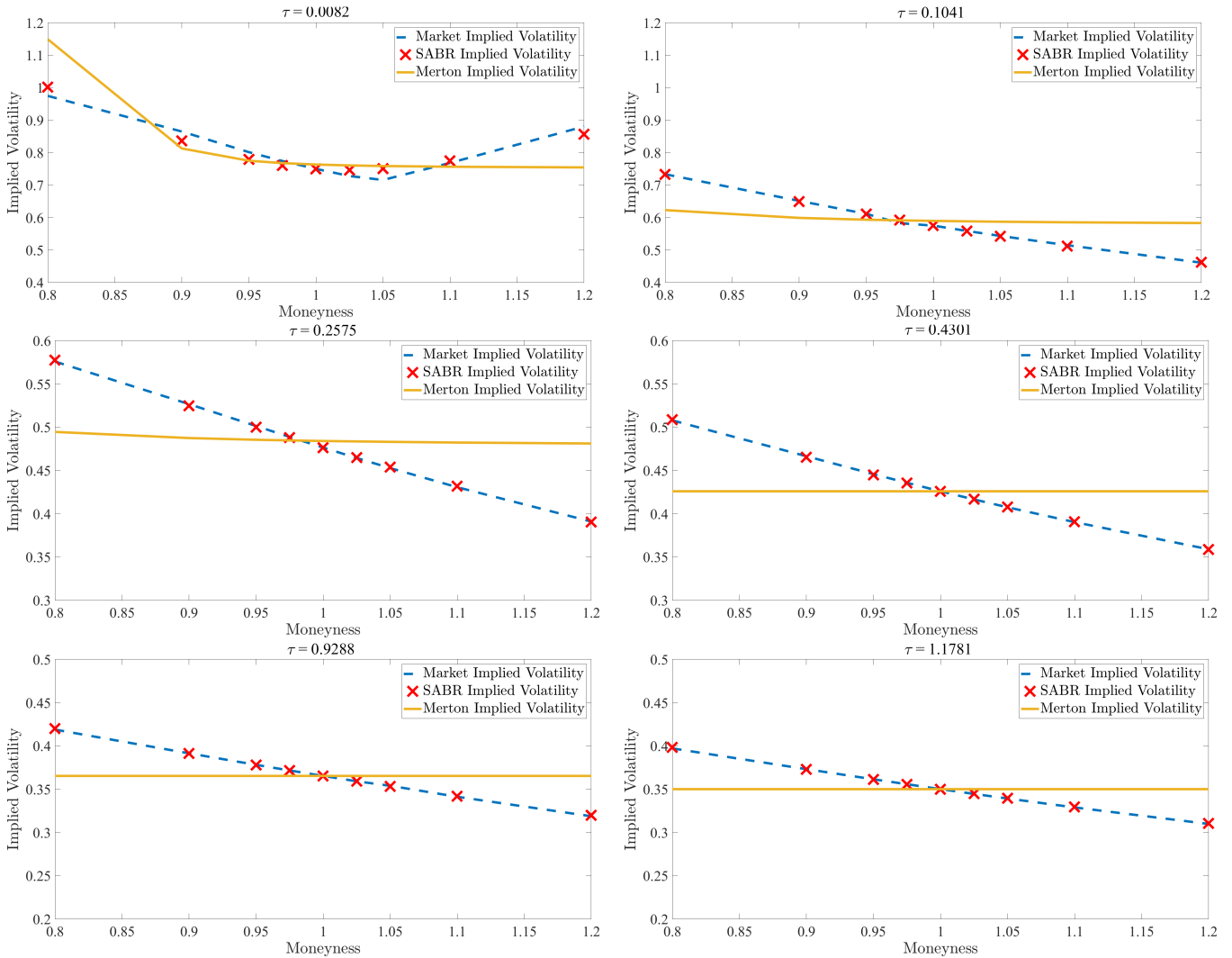


Figure 4.1: The Implied Volatility in S&P 500 Index Options during 2008 Market Crash

From figure 4.1 we know that the SABR implied volatility curves are closer than the market implied volatility. It indicates that SABR model overall calibrates the implied volatility smile and skew better than Merton jump-diffusion model no regardless of short-, mid- and long-term. The Merton calibrated implied volatility tends to display a flat line with increasing time to expiration. It makes sense since the diffusion process dominates the jump process in the long run that makes long-term implied volatility displays a flat line as (Derman and Miller (2016),p385) suggest. Now, we take a look at the calibrated parameter values in SABR and Merton jump-diffusion model.

$\tau$	0.0082	0.1041	0.2575	0.4301	0.9288	1.1781	<i>Mean</i>
$\sigma_0$	0.7499	0.5750	0.4764	0.4259	0.3653	0.3500	0.4904
$\beta$	0.5000	0.5000	0.5000	0.5000	0.5000	0.5000	0.5000
$\rho$	-0.0354	-0.7066	-0.9245	-0.8346	-0.9384	-0.8908	-0.7217
$\xi$	5.1271	1.5489	0.7559	0.6463	0.3394	0.2956	1.4522
<i>RMSE</i>	0.0221	0.0036	0.0012	0.0006	0.0006	0.0005	0.0048

Table 4.1: SABR Estimated Parameters and Errors in S&P 500 Index Options during 2008 Market Crash

By comparing *RMSE* in the table 4.1 and 4.2, each *RMSE* in SABR model is smaller than the Merton jump-diffusion model which indicates the SABR model has a higher calibrated effectiveness than Merton jump-diffusion. Negative  $\rho$  causes a negative volatility skew which consistent with the observed implied volatility curve. However, the volatility of volatility  $\xi$  in short-term implied volatility is 5.1271 and 1.5489 respectively, which are unreasonable large. In fact, SABR model has a hard time generating very steep implied volatility without assuming unreasonable large  $\xi$ . Such steep implied volatility smiles and skews are frequently observed under the market crash period. The extreme value of  $\xi$  makes us doubt the SABR model calibrated effectiveness on short-term implied volatility smile and skew.

$\tau$	0.0082	0.1041	0.2575	0.4301	0.9288	1.1781	<i>Mean</i>
$\sigma_0$	0.7499	0.5750	0.4764	0.4259	0.3653	0.3500	0.4904
$\mu_J$	-0.4210	-0.9991	-0.9791	0.0008	0.0004	0.0003	-0.3996
$\sigma_J$	0.0000	1.4965	1.0258	0.0067	0.0071	0.0071	0.4239
$\lambda$	0.2861	0.0377	0.0129	0.2940	0.5859	0.5401	0.2928
<i>RMSE</i>	0.0768	0.0652	0.0478	0.0409	0.0272	0.0239	0.0469

Table 4.2: Merton Jump-diffusion Estimated Parameters and Errors in S&P 500 Index Options during 2008 Market Crash

In terms of calibrated parameter values in the Merton jump-diffusion model, the mean jump in return  $\mu_J = -39.96\%$  is higher than the historical data. Up to May 4<sup>th</sup>, 2020, the largest daily percentage losses in S&P 500 index is 20.47% and only happen once. If we follow Andersen and Andreasen (2000) interpretation on  $\mu_J$  that  $\mu_J$  represents the investor's future market anticipation. The high  $\mu_J$  indicates that the investors anticipate the future bigger market crash. Furthermore, after October 15, 2008, S&P 500 index fell  $-8.93\%$  on December 1, 2008. The drop of S&P 500 index on that day is another top twenty largest historical daily percentage losses. The estimated jump intensity  $\lambda = 0.2928$  jumps per year seems reasonable if we compare it with the reality.

In our initial assumption, we think that the Merton jump-diffusion model is superior to SABR model in terms of capturing the observed volatility smile and skew under the market crash period. This is because

the background of proposing the Merton jump-diffusion is to solve the volatility smile and skew under the market crash. It may have a strong explanation relative to SABR model under the market crash. However, the empirical results show that SABR model overall calibrates steep implied volatility smile and skew better than the Merton jump-diffusion model at the cost of taking extremely large value on  $\xi$ . In terms of *RMSE*, SABR model overall calibrate the implied volatility curves better than Merton jump-diffusion model in this case.

#### 4.2.2 2020 Market Crash

Analyzing the calibrated effectiveness in the 2020 market crash is the same as the 2008 market crash. We calibrate the implied volatility under the 2020 market crash. We plot the calibrated result in figure 4.2. The corresponding parameters and *RMSE* are presented in table 4.3 and 4.4.

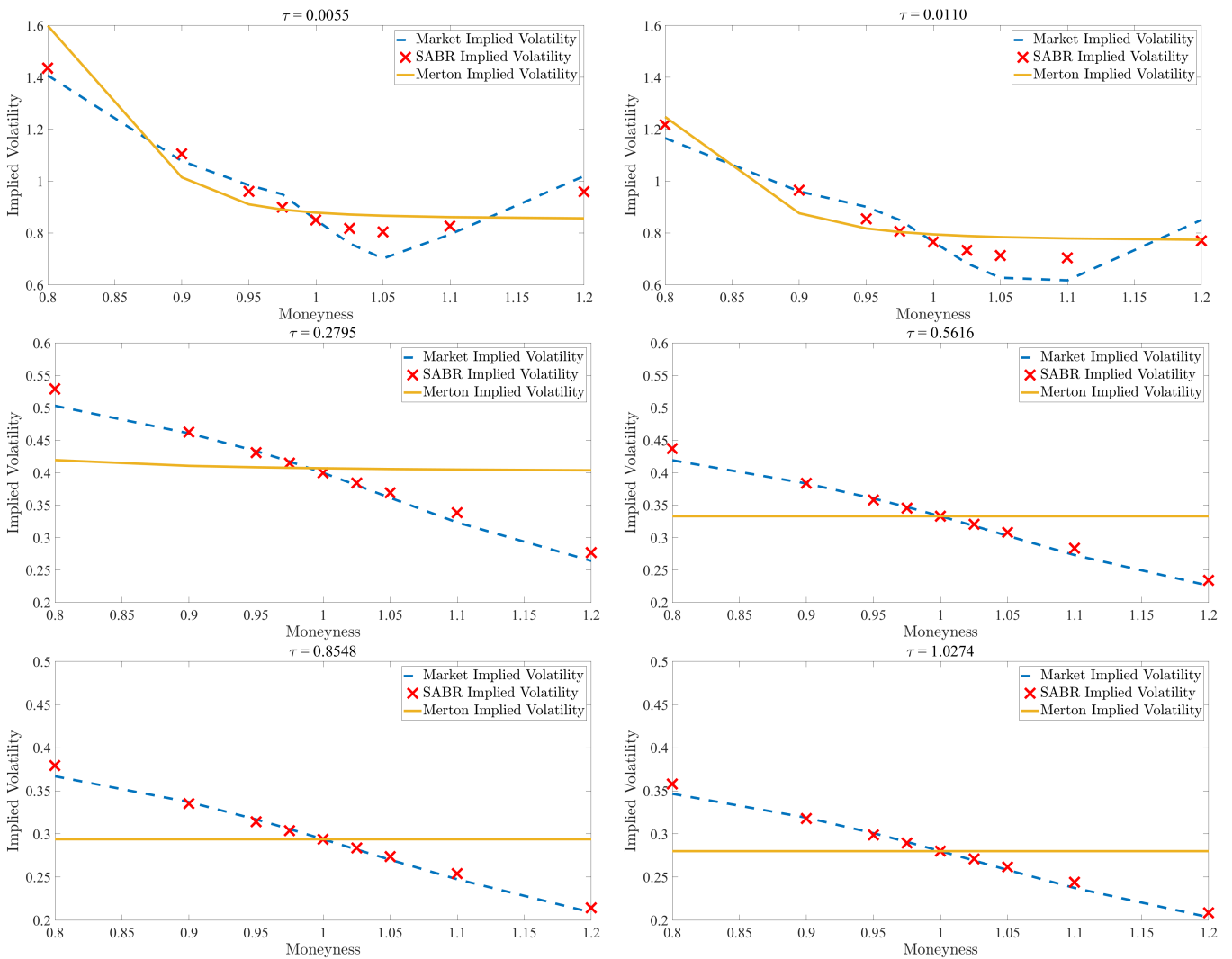


Figure 4.2: The Implied Volatility in S&P 500 Index Options during 2020 Market Crash

Similar to figure 4.1, SABR model again performs better than the Merton jump-diffusion model. Mid- and long-term implied volatility curves tend to be the flat lines in the Merton jump-diffusion model. The calibrated long-term implied volatility values are the constant values in the 2008 and 2020 market crash. <sup>5</sup>.

<sup>5</sup>see table A.3 and A.6

$\tau$	0.0055	0.0110	0.2795	0.5616	0.8548	1.0274	<i>Mean</i>
$\sigma_0$	0.8504	0.7660	0.3997	0.3329	0.2938	0.2800	0.4871
$\beta$	0.5000	0.5000	0.5000	0.5000	0.5000	0.5000	0.5000
$\rho$	-0.3317	-0.4062	-1.0000	-1.0000	-1.0000	-1.0000	-0.7897
$\xi$	8.5143	6.1931	1.0673	0.8638	0.6926	0.6223	2.9922
<i>RMSE</i>	0.0506	0.0581	0.0113	0.0079	0.0054	0.0050	0.0231

Table 4.3: SABR Estimated Parameters and Errors in S&amp;P 500 Index Options during 2020 Market Crash

In table 4.3,  $\xi$  in short-term implied volatility are taken the extreme values, larger than the values in the 2008 market crash. The *RMSE* in each term in SABR model is smaller relative to the Merton jump-diffusion model. It indicates that SABR model calibrates the volatility smile and skew better than Merton jump-diffusion. However,  $\xi$  in short-term implied volatility is also in doubt.

$\tau$	0.0055	0.0110	0.2795	0.5616	0.8548	1.0274	<i>Mean</i>
$\sigma_0$	0.8504	0.7660	0.3997	0.3329	0.2938	0.2800	0.4871
$\mu_J$	-0.5988	-0.9956	-1.0000	-0.0004	-0.0015	-0.0005	-0.4328
$\sigma_J$	0.0996	1.2109	0.7261	0.0066	0.0069	0.0069	0.3428
$\lambda$	0.5610	0.2357	0.0116	0.2407	0.4742	0.5666	0.3483
<i>RMSE</i>	0.1159	0.1008	0.0659	0.0549	0.0446	0.0405	0.0704

Table 4.4: Merton Jump-diffusion Estimated Parameters and Errors in S&amp;P 500 Index Options during 2020 Market Crash

In table 4.4, the mean jump in return  $\mu_J = -43.28\%$  again seems excess when compared to historical data. It is interesting to note that the estimated jump intensity  $\lambda = 0.3483$  jumps per year is lower than what we have observed from the historical data. Up to May 4<sup>th</sup>, 2020, the top twenty daily percentage losses in S&P 500 index, three of them had happened in 2020. The historical data shows that the investors underestimate the frequency of occurring the market crash. However, investors believe that it will trigger the bigger market crash than the one in 1987 if it market crash occurs in the future.

In conclusion, SABR model calibrates the volatility smile and skew better than Merton jump-diffusion in those two market crashes from the views of *RMSE*. However, the calibrated parameters in the short-term implied volatility in SABR model are doubtful.

## 5 Discussion

In this seminar paper, we compare the calibrated effectiveness between the SABR model and the Merton jump-diffusion model during the market crash. The empirical result indicates that the SABR model performs better than Merton jump-diffusion model. In this section, we present several explanations for the result. Firstly, SABR model is a model that calculates the implied volatility directly while Merton jump-diffusion model calculates the implied volatility indirectly. This difference may lead SABR model to do better than Merton jump-diffusion in terms of capturing the implied volatility smile and skew. Secondly, we calibrate two unknown parameters in SABR model and three unknown parameters in Merton jump-diffusion model. As we mentioned in section 4.1, high dimensional space as well as limited data induce inaccurate calibrated

result. One more calibrated parameter may lead Merton jump-diffusion model less efficient than SABR model. What if happen if we calibrate the same numbers of the parameter. This is further research we need to do.

In the paper, we conclude SABR model does better than Merton jump-diffusion model from the views of *RMSE*. However, the calibrated the value of the volatility of volatility in short-term implied volatility is unreasonable large. The extreme value of the calibrated parameter confuses us whether the SABR model is the optimal model under the market crash. Further, we are not sure whether the calibrated parameters are the local optimal or global optimal. Different local calibrated parameter values can lead to different conclusions. Our finding may not persuasive if our estimated parameter values are not global optimal. The global calibration scheme and other convincing option pricing models should be considered in the future.

## 6 Conclusion

After the 1987 market crash, equity index option markets exhibit an implied volatility smile or skew, which challenges the BSM model assumption that the volatility is constant over time. Advanced models like stochastic volatility (SABR model) or Merton jump-diffusion model are proposed to solve the implied volatility smile problem. However, those two models have their advantages and disadvantages. In this seminar paper, we compare those two models in calibrating the observed implied volatility smile and skew during the 2008 and 2020 market crash.

Our empirical result suggests that the SABR model overall calibrates the implied volatility smile and skew better than Merton jump-diffusion model. The mid- and long-term implied volatility displays a flat line in jump-diffusion model. It makes sense since the diffusion process dominates the jump process that makes the implied volatility curve tend to be flat in the long run. However, the value of the volatility of volatility in short-term implied volatility in SABR model is unreasonably large and at odds with reality. In fact, SABR model has a hard time generating very steep volatility skews without assuming the unconvincing the volatility of volatility. Hence, SABR model is suitable to calibrate the mid- and long-term implied volatility in S&P 500 index option under the market crash. In terms of short-term volatility, neither SABR model nor Merton jump-diffusion model explains the implied volatility smile successfully from the perspective of calibrated parameters.

The failure of the stochastic volatility model and the jump-diffusion model in matching the short-term implied volatility in S&P 500 index option under the market crash period encourages us to incorporate the advantages of both models. That is how the stochastic volatility model with jump comes. This kind of models may produce a very steep short-term implied volatility skews without large volatility of volatility. It can also produce a skew for option with long maturities which consistent with the market observation. It forms a starting point for additional research.

## References

- Andersen, L. and J. Andreasen (2000). Jump-diffusion processes: Volatility smile fitting and numerical methods for option pricing. *Review of derivatives research* 4(3), 231–262.
- Black, F. and M. Scholes (1973). The pricing of options and corporate liabilities. *Journal of Political Economy* 81(3), 637–654.
- Bogatyрева, N., R. Grandez, S. Rodríguez Apolinar, and A. Soldevilla (2019). Sabr: a stochastic volatility model in practice.
- Camlibel, M. and J. Lundgren (2010). *Investigation of the effect of using stochastic and local volatility when pricing barrier options*.
- Christie, A. A. (1982). The stochastic behavior of common stock variances: Value, leverage and interest rate effects. *Journal of Financial Economics* 10(4), 407–432.
- Derman, E. and M. B. Miller (2016). *The volatility smile*. Wiley finance. Hoboken, New Jersey: John Wiley Sons, Inc.
- Gatheral, J. (2011). *The volatility surface: a practitioner’s guide*, Volume 357. John Wiley & Sons.
- Hagan, P., D. Kumar, A. Lesniewski, and D. Woodward (2002, 01). Managing smile risk. *Wilmott Magazine* 1, 84–108.
- Huang, K. (2019). *Implied Volatility and Option Pricing Models*. Ph. D. thesis, Finland.
- Hull, J. (2013). *Options, Futures and Other Derivatives: QMUL* (8. ed. ed.). Pearson Education UK.
- Kovachev, Y. (2014). Calibration of stochastic volatility models.
- Lewis, A. L. (2001). A simple option formula for general jump-diffusion and other exponential lévy processes. *Available at SSRN 282110*.
- Merton, R. C. (1973). Theory of rational option pricing. *The Bell Journal of economics and management science*, 141–183.
- Merton, R. C. (1976). Option pricing when underlying stock returns are discontinuous. *Journal of Financial Economics* 3(1), 125–144.
- Weiqi, Y. (2020). Modeling the Volatility Smile from Traditional and Behavioral Finance Perspectives - Empirical Evidence from S&P 500 and China 50 ETF Index Options. In *University of Copenhagen*, Master Thesis.
- West, G. (2005). Calibration of the sabr model in illiquid markets. *Applied Mathematical Finance* 12(4), 371–385.



## A Appendix

### A.1 Proof of Implied volatility under ATM option in SABR model

Recall the implied volatility  $\sigma^{iv}(S_t, K)$  in Hagan et al. (2002) is given by:

$$\begin{aligned}\sigma^{iv}(S, K) &= \frac{\sigma_0 \left( 1 + \left( \frac{(1-\beta)^2 \sigma^2}{24(SK)^{1-\beta}} + \frac{\rho\beta\xi\sigma}{4(SK)^{\frac{(1-\beta)}{2}}} + \frac{2-3\rho^2}{24}\xi^2 \right) \tau \right) z}{(SK)^{\frac{(1-\beta)}{2}} \left[ 1 + \frac{(1-\beta)^2}{24} \log^2 \frac{S}{K} + \frac{(1-\beta)^4}{1920} \log^4 \frac{S}{K} + \dots \right] \chi(z)} + \dots \\ z &= \frac{\xi}{\sigma_0} (SK)^{\frac{(1-\beta)}{2}} \log \frac{S}{K} \\ \chi(z) &= \log \left( \frac{\sqrt{1-2\rho z + z^2} + z - \rho}{1 - \rho} \right)\end{aligned}\tag{A.1}$$

We don't take the omitted terms “+...” into account since they are so small that does not have significant impact on the results. When the call option is ATM ( $S = K$ ),  $z$  and  $\chi(z)$  are removed from the equation A.1, then  $\frac{z}{\chi(z)} = 1$ . The equation A.1 now becomes:

$$\begin{aligned}\sigma^{iv}(S, K) &= \frac{\sigma_0 \left( 1 + \left( \frac{(1-\beta)^2 \sigma^2}{24(S^2)^{1-\beta}} + \frac{\rho\beta\xi\sigma}{4(S^2)^{\frac{(1-\beta)}{2}}} + \frac{2-3\rho^2}{24}\xi^2 \right) \tau \right)}{(S^2)^{\frac{(1-\beta)}{2}} \left[ 1 + \frac{(1-\beta)^2}{24} \log^2 \frac{S}{S} + \frac{(1-\beta)^4}{1920} \log^4 \frac{S}{S} \right]} \\ &= \frac{\sigma_0 \left( 1 + \left( \frac{(1-\beta)^2 \sigma^2}{24S^{2-2\beta}} + \frac{\rho\beta\xi\sigma}{4S^{1-\beta}} + \frac{2-3\rho^2}{24}\xi^2 \right) \tau \right)}{S^{1-\beta}}\end{aligned}\tag{A.2}$$

### A.2 Proof of PIDE in Merton Jump-diffusion model

In this part, we try to derivate the PIDE in Merton Jump-diffusion model based on (Derman and Miller (2016),p395). Recall that the dynamics of underlying asset price  $S_t$  is

$$\frac{dS_t}{S_t} = \mu dt + \sigma dW_t + J dq_t\tag{A.3}$$

where

$$E[dq_t] = \lambda dt \quad \text{Var}[dq_t] = \lambda dt\tag{A.4}$$

Similar to derivate the PDE in BSM model, in order to derive the option pricing equation in jump-diffusion model, we need to construct a riskless portfolio. To set up a portfolio  $\Pi$ , we long the call option  $C$  and short  $\alpha$  of the underlying asset  $S$ ,

$$\Pi = C - \alpha S\tag{A.5}$$

By Ito's lemma, the dynamics of portfolio  $\Pi$  is given as :

$$\begin{aligned}
d\Pi &= dC - \alpha dS \\
&= \left( \frac{\partial C}{\partial t} + \frac{1}{2} \frac{\partial^2 C}{\partial S^2} \sigma^2 S^2 \right) dt + \left( \frac{\partial C}{\partial S} - \alpha \right) (\mu dS + \sigma S dW) \\
&\quad + [C(S + JS, T) - C(S, t) - \alpha JS] dq
\end{aligned} \tag{A.6}$$

To make the portfolio instantaneously risk-less, we need to eliminate the  $dS$ ,  $d\sigma$  and  $dq$  terms. However, we cannot eliminate all the risk by choosing  $\alpha$ . If we hedge  $dS$  and  $d\sigma$  term, then  $dq$  term leaves and vice versa. We decide only to hedge the diffusion part of the underlying asset which means we make  $\alpha = \frac{\partial C}{\partial S}$ . Hence,  $d\Pi$  reduces to

$$d\Pi = \left( \frac{\partial C}{\partial t} + \frac{1}{2} \frac{\partial^2 C}{\partial S^2} \sigma^2 S^2 \right) dt + \left[ C(S + JS, T) - C(S, t) - \frac{\partial C}{\partial S} JS \right] dq \tag{A.7}$$

Even we have hedge the risk of  $dS$  and  $d\sigma$  term, jump risk ( $dq$  term) still exist in equation A.7. Under no-arbitrage condition, hedged portfolio should only earn risk-free return. In other words, we need to cancel out the jump risk. In order to hedge jump risk, we assume jump is diversifiable. Hence, jump carries no risk premium. Averaging over all possible jumps, we finally can get the risk-less portfolio:

$$\begin{aligned}
E[d\Pi] &= \left( \frac{\partial C}{\partial t} + \frac{1}{2} \frac{\partial^2 C}{\partial S^2} \sigma^2 S^2 \right) dt + E \left[ C(S + JS, T) - C(S, t) - \frac{\partial C}{\partial S} JS \right] E[dq] \\
&= r\Pi dt
\end{aligned} \tag{A.8}$$

Putting equation A.4, A.5 and  $\alpha = \frac{\partial C}{\partial S}$  into A.8 and rearranging it, we get the pricing partial integro-differential equation.

$$\frac{\partial C}{\partial t} + \frac{1}{2} \frac{\partial^2 C}{\partial S^2} \sigma^2 S^2 + \frac{\partial C}{\partial S} rS - rC + \lambda E \left[ C(S + JS, T) - C(S, t) - \frac{\partial C}{\partial S} JS \right] = 0 \tag{A.9}$$

### A.3 Proof of Characteristic Function for Merton Jump-diffusion Model

In this part, we derive the characteristic function for Merton jump-diffusion model based on (Gatheral (2011),p56) works. Recall that the dynamics of underlying asset price  $S_t$  under the Merton jump-diffusion model is given as:

$$\frac{dS_t}{S_t} = \mu dt + \sigma dW_t + J dq_t \tag{A.10}$$

In (Gatheral (2011),p56) comment, the logarithmic version of Merton jump-diffusion model follows the Lévy process. Denote the forward price  $F = S_0 e^{r\tau}$  and  $x_\tau = \log \frac{S_\tau}{F}$ . If  $x_\tau$  is a Lévy process with Lévy density  $v(\chi)$ , its characteristic function  $f_\tau^{Merton}(\phi) = E[e^{i\phi x_\tau}]$  has the Lévy-Khintchine representation:

$$f_\tau^{Merton}(\phi) = \exp \left\{ i\chi w\tau - \frac{1}{2} \phi^2 \sigma^2 \tau + \tau \int [e^{i\phi \chi} - 1] v(\chi) d\chi \right\} \tag{A.11}$$

In the Merton jump-diffusion model, the Lévy density  $v(\chi)$  is given as:

$$v(\chi) = \frac{\lambda}{\sqrt{2\pi}\sigma_J} \exp \left\{ -\frac{\left( \chi - \left( \log(1 + \mu_J) - \frac{\sigma_J^2}{2} \right) \right)^2}{2\sigma_J^2} \right\} \quad (\text{A.12})$$

Putting equation A.12 into equation A.11, we have:

$$\begin{aligned} f_\tau^{Merton}(\phi) &= \exp \left\{ i\phi w\tau - \frac{1}{2}\phi^2\sigma^2\tau + \tau \int [e^{i\phi\chi} - 1] \frac{\lambda}{\sqrt{2\pi}\sigma_J} \exp \left\{ -\frac{\left( \chi - \left( \log(1 + \mu_J) - \frac{\sigma_J^2}{2} \right) \right)^2}{2\sigma_J^2} \right\} d\chi \right\} \\ &= \exp \left\{ i\phi w\tau - \frac{1}{2}\phi^2\sigma^2\tau + \lambda\tau \left( e^{i\phi \left( \log(1 + \mu_J) - \frac{\sigma_J^2}{2} \right) - \frac{\phi^2\sigma_J^2}{2}} - 1 \right) \right\} \end{aligned} \quad (\text{A.13})$$

In order to get the drift parameter  $\omega$ , we make the expectation of the underlying asset prices equals to the forward price. In (Gatheral (2011),p56), it can be written as

$$f_\tau^{Merton}(-i) = E[e^{x_\tau}] = 1 \quad (\text{A.14})$$

where  $\phi = -i$ , Putting equation A.14 into equation A.13, we have

$$f_\tau^{Merton}(-i) = \exp \left\{ -i^2 w\tau - \frac{1}{2}\sigma^2\tau + \lambda\tau \left( e^{-i^2 \left( \log(1 + \mu_J) - \frac{\sigma_J^2}{2} \right) + \frac{\sigma_J^2}{2}} - 1 \right) \right\} = 1 \quad (\text{A.15})$$

Recall that  $i$  is a unit imaginary number which has  $i^2 = -1$ . Putting  $i^2 = -1$  into equation A.15, and equation A.15 becomes:

$$\exp \left\{ w\tau + \frac{1}{2}\sigma^2\tau + \lambda\tau \left( e^{\left( \log(1 + \mu_J) - \frac{\sigma_J^2}{2} \right) + \frac{\sigma_J^2}{2}} - 1 \right) \right\} = 1 \quad (\text{A.16})$$

Taking logs for each side, and then we get the expression for  $w$ :

$$w = -\frac{1}{2}\sigma^2 - \lambda \left( e^{\left( \log(1 + \mu_J) - \frac{\sigma_J^2}{2} \right) + \frac{\sigma_J^2}{2}} - 1 \right) \quad (\text{A.17})$$

#### A.4 Proof of Pricing Formula for Merton Jump-diffusion Model

In this part, we derive the pricing formula for Merton jump-diffusion model based on (Gatheral (2011),p59) work. (Gatheral (2011),p59) take the covered call position to illustrate how to derive the pricing formula. Covered call position is a trading strategy that the stockholder sells its corresponding numbers of call options. When the stock price rise but still below the strike price (OTM), the option writer will benefit from the stock price rising and the option premium. However, when the option is ITM, the option writer loses the gain

from the price rising and merely receives the option premium. In short, the covered call position is a trading strategy that makes the stockholder get the fixed option premium at the cost of giving up the potential of stock increasing. The payoff of the covered call position is given as:

$$\text{payoff} = \min[S_T, K] \quad (\text{A.18})$$

Define the Fourier transform of this kind of covered call position  $G(k, \tau)$  with respect to  $k$ , where  $k = \log(\frac{K}{F})$ :

$$\hat{G}(\chi, \tau) = \int_{-\infty}^{+\infty} e^{i\chi k} G(k, \tau) dk \quad (\text{A.19})$$

Recall that  $\tau$  is the time to expiration  $\tau = T - t$ . Gatheral (2011),p59) assumes that the zero risk-free rate and no dividends during the derivation.

$$\begin{aligned} \frac{1}{S} \hat{G}(\chi, T - t) &= \int_{-\infty}^{+\infty} e^{i\chi k} E \left[ \min(e^{x_T}, e^k)^+ | x_t = 0 \right] dk \\ &= E \left[ \int_{-\infty}^{+\infty} e^{i\chi k} \min(e^{x_T}, e^k)^+ dk | x_t = 0 \right] \\ &= E \left[ \int_{-\infty}^{x_T} e^{i\chi k} e^k dk + \int_{x_T}^{+\infty} e^{i\chi k} e^{x_T} dk | x_t = 0 \right] \\ &= E \left[ \frac{e^{(1+i\chi)x_T}}{1+i\chi} - \frac{e^{(1+i\chi)x_T}}{i\chi} | x_t = 0 \right] \quad \text{if } 0 < \text{Im}[\chi] < 1 \\ &= E \left[ \frac{e^{(1+i\chi)x_T} (i\chi) - e^{(1+i\chi)x_T} (1+i\chi)}{(1+i\chi)(i\chi)} | x_t = 0 \right] \\ &= \frac{1}{\chi(\chi - i)} E \left[ e^{(1+i\chi)x_T} | x_t = 0 \right] \\ &= \frac{1}{\chi(\chi - i)} f_T^{\text{Merton}}(\chi - i) \end{aligned} \quad (\text{A.20})$$

where we use  $i^2 = -1$  and  $f_T^{\text{Merton}}(\chi - i) = E[e^{(1+i\chi)x_T} | x_t = 0]$ <sup>6</sup> to derive equation A.20. Also, we should note that the payoff of covered call position is  $\min[S_T, K]$ .  $\int_{-\infty}^{x_T} e^{i\chi k} e^k dk$  represents the option writer's payoff when the stock price rise but still below the strike price (OTM) and  $\int_{x_T}^{+\infty} e^{i\chi k} e^{x_T} dk$  is the payoff that the stock price rising and the option is ITM.  $\text{Im}[\chi]$  is the function that try to return the imaginay part of  $\chi$ .

To get the call price from the views of the characteristic function, (Gatheral (2011),p59) expresses it in terms of covered call, inverts the Fourier transform, set  $\text{Im}[\chi] = \frac{1}{2}$  and does the integration. We finally have:

<sup>6</sup>Recall that in appendix A.3, we have  $f_\tau^{\text{Merton}}(\chi) = E[e^{i\chi x_\tau}]$ , we replace  $\tau$  with  $T$  and  $\chi$  with  $\chi - i$ , and then we can get  $f_T^{\text{Merton}}(\chi - i) = E[e^{(1+i\chi)x_T} | x_t = 0]$

$$\begin{aligned}
C_{JD} &= S - S \frac{1}{2\pi} \int_{-\infty + \frac{i}{2}}^{\infty + \frac{i}{2}} \frac{d\chi}{\chi(\chi - i)} f_T^{Merton}(\chi - i) e^{-ik\chi} \\
&= S - S \frac{1}{2\pi} \int_{-\infty}^{\infty} \frac{d\chi}{(\chi + \frac{i}{2})(\chi - \frac{i}{2})} f_T^{Merton} \left( \chi - \frac{i}{2} \right) e^{-ik(\chi + \frac{i}{2})} \\
&= S - \sqrt{SK} \frac{1}{\pi} \int_0^{\infty} \frac{d\chi}{\chi^2 + \frac{1}{4}} \operatorname{Re} \left[ e^{-i\chi k} f^{Merton} \left( \phi = \left( \chi - \frac{i}{2} \right) \right) \right]
\end{aligned} \tag{A.21}$$

where  $k = \log(\frac{K}{S})$ . Again, (Gatheral (2011), p59) assume zero interest rate to derive the option price under Merton jump-diffusion model. We need discount equation A.21 to get the equation we use in the empirical analysis.

$$C_{JD} = e^{-r\tau} \left\{ S - \sqrt{SK} \frac{1}{\pi} \int_0^{\infty} \frac{d\chi}{\chi^2 + \frac{1}{4}} \operatorname{Re} \left[ e^{-i\chi k} f^{Merton} \left( \phi = \left( \chi - \frac{i}{2} \right) \right) \right] \right\} \tag{A.22}$$

## A.5 2008 Market Crash Original Data

Expiration \ Moneyness	0.8	0.9	0.95	0.975	1	1.025	1.05	1.1	1.2
0.0082	0.9747	0.8648	0.8013	0.7741	0.7499	0.7278	0.7156	0.7682	0.8805
0.1041	0.7333	0.6512	0.6112	0.5825	0.5750	0.5586	0.5432	0.5146	0.4607
0.2575	0.5758	0.5266	0.5013	0.4887	0.4764	0.4643	0.4527	0.4306	0.3909
0.4301	0.5078	0.4664	0.4457	0.4357	0.4259	0.4165	0.4074	0.3903	0.3589
0.9288	0.4188	0.3914	0.3781	0.3716	0.3653	0.3591	0.3539	0.3412	0.3187
1.1781	0.3971	0.3731	0.3614	0.3557	0.3500	0.3445	0.3392	0.3289	0.3098

Table A.1: Market Implied Volatilities of European Call Options on the S&P 500 Index, as of October 15, 2008 18:08 spot price: 907.84 and risk free rate : 4.55%.

### A.5.1 Calibrated SABR Data

Expiration \ Moneyness	0.8	0.9	0.95	0.975	1	1.025	1.05	1.1	1.2
0.0082	1.0014	0.8357	0.7791	0.7606	0.7497	0.7465	0.7504	0.7747	0.8569
0.1041	0.7327	0.6489	0.6107	0.5925	0.5750	0.5581	0.5419	0.5118	0.4620
0.2575	0.5775	0.5246	0.5000	0.4880	0.4763	0.4649	0.4537	0.4318	0.3904
0.4301	0.5086	0.4651	0.4450	0.4354	0.4259	0.4168	0.4078	0.3906	0.3586
0.9288	0.4200	0.3912	0.3779	0.3715	0.3653	0.3592	0.3532	0.3417	0.3199
1.1781	0.3982	0.3728	0.3611	0.3555	0.3500	0.3447	0.3394	0.3294	0.3105

Table A.2: SABR Implied Volatilities of European Call Options on the S&P 500 Index, as of October 15, 2008 18:08 spot price: 907.84 and risk free rate : 4.55%.

### A.5.2 Calibrated Merton Jump-diffusion Data

Expiration \ Moneyness	0.8	0.9	0.95	0.975	1	1.025	1.05	1.1	1.2
0.0082	1.1491	0.8127	0.7749	0.7676	0.7632	0.7605	0.7586	0.7564	0.7543
0.1041	0.6228	0.5988	0.5932	0.5912	0.5896	0.5882	0.5870	0.5852	0.5829
0.2575	0.4945	0.4874	0.4854	0.4847	0.4840	0.4835	0.4830	0.4822	0.4811
0.4301	0.4259	0.4259	0.4259	0.4259	0.4259	0.4259	0.4259	0.4259	0.4259
0.9288	0.3653	0.3653	0.3653	0.3653	0.3653	0.3653	0.3653	0.3653	0.3653
1.1781	0.3500	0.3500	0.3500	0.3500	0.3500	0.3500	0.3500	0.3500	0.3500

Table A.3: Merton Implied Volatilities of European Call Options on the S&P 500 Index, as of October 15, 2008 18:08 spot price: 907.84 and risk free rate : 4.55%.

## A.6 2020 Market Crash Original Data

Expiration \ Moneyness	0.8	0.9	0.95	0.975	1	1.025	1.05	1.1	1.2
0.0055	1.4074	1.0771	0.9843	0.9493	0.8504	0.7602	0.7015	0.7947	1.0194
0.0110	1.1655	0.9603	0.9009	0.8500	0.7660	0.6828	0.6277	0.6176	0.8506
0.2795	0.5032	0.4607	0.4334	0.4174	0.3997	0.3808	0.3613	0.3233	0.2641
0.5616	0.4192	0.3834	0.3603	0.3471	0.3329	0.3180	0.3027	0.2730	0.2259
0.8548	0.3668	0.3369	0.3168	0.3056	0.2938	0.2819	0.2700	0.2474	0.2090
1.0274	0.3465	0.3188	0.3008	0.2907	0.2800	0.2691	0.2582	0.2373	0.2034

Table A.4: Market Implied Volatilities of European Call Options on the S&P 500 Index, as of March 9, 2020  
21:00 spot price: 2745.36 and risk free rate : 0.77%.

### A.6.1 Calibrated SABR Data

Expiration \ Moneyness	0.8	0.9	0.95	0.975	1	1.025	1.05	1.1	1.2
0.0055	1.4357	1.1049	0.9605	0.8993	0.8501	0.8175	0.8041	0.8269	0.9597
0.0110	1.2172	0.9653	0.8551	0.8070	0.7658	0.7337	0.7127	0.7044	0.7704
0.2795	0.5292	0.4626	0.4308	0.4151	0.3996	0.3843	0.3690	0.3385	0.2767
0.5616	0.4374	0.3836	0.3579	0.3453	0.3328	0.3204	0.3081	0.2836	0.2342
0.8548	0.3794	0.3352	0.3142	0.3039	0.2937	0.2837	0.2737	0.2539	0.2144
1.0274	0.3580	0.3177	0.2986	0.2893	0.2800	0.2709	0.2618	0.2439	0.2084

Table A.5: SABR Implied Volatilities of European Call Options on the S&P 500 Index, as of March 9, 2020  
21:00 spot price: 2745.36 and risk free rate : 0.77%.

### A.6.2 Calibrated Merton Jump-diffusion Data

Expiration \ Moneyness	0.8	0.9	0.95	0.975	1	1.025	1.05	1.1	1.2
0.0055	1.5987	1.0144	0.9105	0.8901	0.8784	0.8713	0.8667	0.8613	0.8565
0.0110	1.2473	0.8761	0.8176	0.8037	0.7947	0.7887	0.7844	0.7791	0.7739
0.2795	0.4195	0.4106	0.4084	0.4076	0.4069	0.4063	0.4057	0.4049	0.4038
0.5616	0.3329	0.3329	0.3329	0.3329	0.3329	0.3329	0.3329	0.3329	0.3329
0.8548	0.2938	0.2938	0.2938	0.2938	0.2938	0.2938	0.2938	0.2938	0.2938
1.0274	0.2800	0.2800	0.2800	0.2800	0.2800	0.2800	0.2800	0.2800	0.2800

Table A.6: Merton Implied Volatilities of European Call Options on the S&P 500 Index, as of March 9, 2020  
21:00 spot price: 2745.36 and risk free rate : 0.77%.